

# Nanosecond Metal-to-Ligand Charge Transfer State in an Fe(II) Chromophore: Lifetime Enhancement via Nested Potentials

Justin Malme<sup>1‡</sup>, Reese A. Clendening<sup>2‡</sup>, Ryan Ash<sup>1</sup>, Tong Ren<sup>2\*</sup> and Josh Vura-Weis<sup>1\*</sup>

<sup>1</sup> Department of Chemistry, University of Illinois at Urbana–Champaign, Urbana, Illinois 61801

<sup>2</sup> Department of Chemistry, Purdue University, West Lafayette, Indiana 47907, United States

**KEYWORDS.** Charge transfer, Fe(II) chromophore, long lifetime, earth abundant, tetragonal symmetry, nested potential energy surfaces

**ABSTRACT:** Examples of Fe complexes with long-lived ( $\geq 1$  ns) charge-transfer states are limited to pseudo-octahedral geometries with strong  $\sigma$ -donor chelates. Alternative strategies based on varying both coordination motifs and ligand donicity are highly desirable. Reported herein is an air-stable, tetragonal Fe<sup>II</sup> complex, Fe(HMTI)(CN)<sub>2</sub> (HMTI = 5,5,7,12,12,14-hexamethyl-1,4,8,11-tetraazacyclotetradeca-1,3,8,10-tetraene) with a 1.25 ns metal-to-ligand charge transfer (MLCT) lifetime. The structure has been determined, and the photophysical properties examined in a variety of solvents. The HMTI ligand is highly  $\pi$ -acidic due to low lying  $\pi^*(C=N)$ , which enhances  $\Delta_{Fe}$  via stabilizing  $t_{2g}$  orbitals. The inflexible geometry of the macrocycle results in short Fe–N bonds, and density functional theory calculations show that this rigidity results in an unusual set of nested potential energy surfaces. Moreover, the lifetime and energy of the MLCT state depends strongly on the solvent environment. This dependence is caused by modulation of the axial ligand-field strength by Lewis acid-base interactions between the solvent and the cyano ligands. This work represents the first example of a long-lived charge transfer state in an Fe<sup>II</sup> macrocyclic species.

In recent years, an intense interest has arisen in the development of chromophores based on 3d metals,<sup>1–3</sup> which may replace the established chromophores based on Ru or Ir in applications such as dye-sensitized solar cells<sup>4</sup> and photo-redox catalysis.<sup>5</sup> Among 3d metals being studied, iron complexes are most investigated, and frequently compared with their group 8 congeners (*i.e.* Ru).<sup>6</sup> In the case of Ru<sup>II</sup>-based chromophores, the large ligand field splitting ( $\Delta_{Ru}$ ) stabilizes the triplet metal-to-ligand charge transfer state (<sup>3</sup>MLCT) compared to the metal centered excited states (<sup>3</sup>5MC) and hence extends the <sup>3</sup>MLCT lifetime. Analogous ligand field splittings in iron complexes ( $\Delta_{Fe}$ ) are much smaller, promoting rapid deactivation of <sup>3</sup>MLCT via <sup>3</sup>5MC.

The common approaches to increasing  $\Delta_{Fe}$  focus on the modification of classical chelating bipyridine and terpyridine motifs, increasing  $\sigma$ -donicity (*via* C-metallation, carbene or amido moieties), enhancing  $\pi$ -acidity, or intensifying both  $\sigma$ -donicity and  $\pi$ -acidity using mesoionic carbenes.<sup>6,7</sup> Notable successes include Fe<sup>II</sup> complexes with MLCT-type lifetimes of 0.528 ns (A, Figure 1),<sup>8</sup> 3 ns (B)<sup>9,10</sup> or 1 ns (C),<sup>11</sup> and Fe<sup>III</sup> species with ligand-to-metal charge transfer (LMCT) lifetimes up to 2.0 ns.<sup>12</sup> Coordination geometries of Fe complexes with long lived charge-transfer states are limited to *pseudo*-octahedral based on tris-bidentate, bis-tridentate, and tridentate scorpionate chelate motifs.

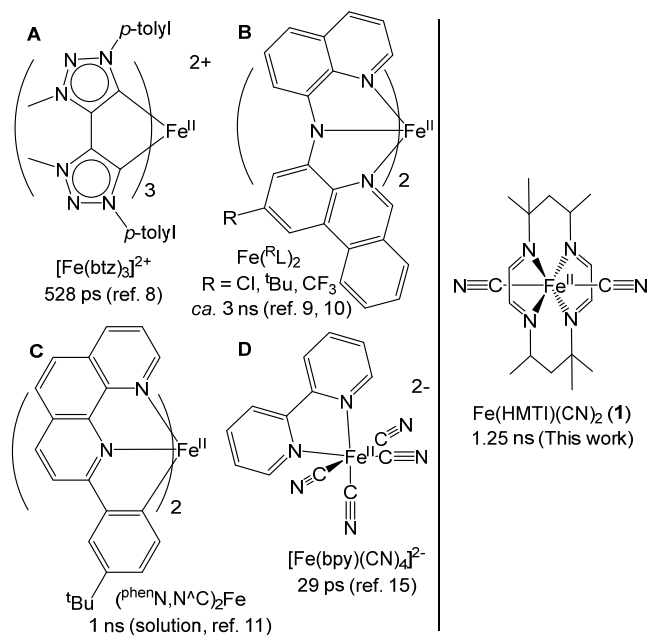


Figure 1. Illustration of selected Fe<sup>II</sup> chromophores (left) and **1** (right).

A complementary approach towards enhancing the lifetime involves heteroleptic or “modular” complexes,<sup>13,14</sup> in which bidentate or tridentate chelates (which act as the charge acceptors for MLCT) are combined with some other ligands. The lifetimes of the resulting complexes have

shown improvement over simple symmetric analogs (e.g. Figure 1, D),<sup>13-15</sup> but have been generally limited to *circa* 10 ps. While the utility of these approaches has been amply demonstrated, it is desirable to expand the library of available coordination motifs for Fe chromophores. Reported in this contribution is a demonstration of the enhancement of  $\Delta_{Fe}$  within a *tetragonal* motif using a  $\pi$ -acidic tetradentate macrocycle, which leads to an Fe<sup>II</sup> species possessing a remarkably long-lived MLCT state.

During the process of investigating the chemistry of Fe<sup>III</sup>(HMC) alkynyls (HMC = 5,5,7,12,12,14-hexamethyl-1,4,8,11-tetraazacyclotetradecane), we re-discovered the conversion of Fe(HMC) compounds to Fe(HMTI) species (HMTI = 5,5,7,12,12,14-hexamethyl-1,4,8,11-tetraazacyclotetradeca-1,3,8,10-tetraene) *via* aerobic dehydrogenation of the HMC ring,<sup>16</sup> a process previously described by Busch and coworkers.<sup>17,18</sup> Inspired by the possibilities of a tetragonally distorted ligand field, we examined the physical attributes of cyano adduct, Fe<sup>II</sup>(HMTI)(CN)<sub>2</sub> (**1**; Figure 1) (see Supporting Information [SI] for synthetic details). The structure of **1** was determined via X-ray diffraction (Figure S1), confirming the two  $\alpha$ -diimine units within the macrocycle bound to the metal center. This results in short Fe-N bonds (1.918(2)-1.939(2) Å) compared to similar polypyridyl-based complexes (Table S1)<sup>19-22</sup> and a planar Fe-macrocycle core, with the N=C-C=N dihedral  $<1^\circ$ . The cyano ligands are oriented *trans* to one another, with an elongated Fe-C bond (1.955(3)Å).<sup>20</sup> More striking is the intense band in the absorption spectra centered at 647 nm (dichloromethane;  $\epsilon=8000\text{ M}^{-1}\text{cm}^{-1}$ ), which is ascribed to MLCT from Fe  $d\pi$  to  $\pi^*(\alpha\text{-diimine})$  (Figure S3).<sup>18</sup> Therefore, femtosecond UV/Visible transient absorption spectroscopy was used to probe the dynamics of the state formed via excitation of this band.

Figure 2 shows selected transient spectra in CHCl<sub>3</sub> after excitation at 636 nm, with kinetic traces at 535 nm and 605 nm shown in the inset. Similar spectral features are observed across various solvents (given in the SI), though as discussed below the lifetimes differ significantly. A prominent ground state bleach (GSB) is centered around 590-640 nm in all solvents, with an excited state absorption (ESA<sub>2</sub>) directly to the blue, centered around 505-530 nm. This band consists of excitations of mixed cyanide-tetraimine ligand-to-metal charge transfer character, as assigned in Figures S9-10. Another ESA (ESA<sub>1</sub>) can be seen in the near-UV from a mix of  $\pi\text{-}\pi^*$  and LMCT transitions, and a third ESA is observed directly to the red of the GSB in the near-IR (ESA<sub>3</sub>) due to low-lying LMCT excitations. These features sharpen slightly in the first 20 ps due to vibrational relaxation, then decay with an exponential time constant of  $1.25 \pm 0.04\text{ ns}$ .

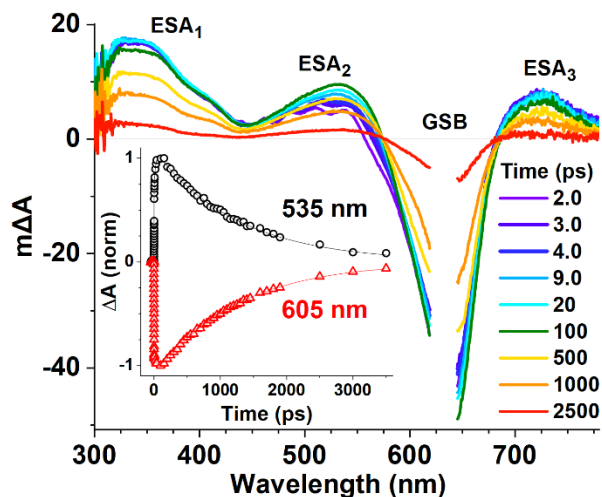


Figure 2. Transient absorption difference spectra at multiple time delays of Fe(HMTI)(CN)<sub>2</sub> in CHCl<sub>3</sub>; Inset shows kinetics traces. Pump scatter (619-645 nm) has been removed.

This nanosecond excited state is assigned as a MLCT state on the basis of spectroelectrochemistry and density functional theory calculations. Fe(HMTI)(CN)<sub>2</sub> has a reversible Fe<sup>III/II</sup> oxidation at 0.14 V (versus the ferrocene couple) and an irreversible ligand-centered reduction at -1.84 V. The oxidation is significantly more anodic than typical Fe<sup>II</sup> chromophores with nanosecond lifetimes (-0.61 to -0.88 V),<sup>9-11</sup> indicating a very electron-poor metal center in the case of **1**. As a result, **1** is exceptionally air stable (see SI). A simulated transient absorption spectrum generated from the spectra of the electrochemically oxidized/reduced complex is an excellent match with the observed transient absorption spectrum,<sup>23</sup> indicating that the long-lived state is of MLCT character ((Spectro)electrochemical section of the SI).

Density functional theory calculations were performed in the Gaussian 16<sup>24</sup> and ORCA 4.2.1<sup>25</sup> packages at the Mo6L/6-311g(d) level of theory<sup>26-29</sup> using a polarizable continuum solvent model<sup>30</sup> for CH<sub>2</sub>Cl<sub>2</sub>. The geometry of the possible singlet, triplet, and quintet spin states was optimized (See SI for details). The singlet is the ground-state and the lowest excited state was found to be a <sup>3</sup>MLCT state at 0.96 eV, corroborating the assignment of the long-lived state from spectroelectrochemistry. The lowest quintet state is at 1.35 eV, featuring a highly distorted puckered ring geometry.

To understand the nanosecond lifetime, we mapped the excited-state potentials using time-dependent density functional theory (TD-DFT). A vibrational mode calculated at 347.4 cm<sup>-1</sup> was selected to model the potential energy surfaces as it had both large symmetric Fe-C displacement as well as symmetric Fe-N displacement in the form of expansion along a single N-Fe-N axis. These symmetric M-L displacements usually correspond with occupation of e<sub>g</sub><sup>\*</sup> orbitals in metal-centered states, as the electron density of these orbitals often lies along the bond coordinate. Eight geometries were generated by vectorizing this vi-

brational mode and adding or subtracting multiples of the vector to the singlet ground state geometry. Singlet and triplet single-point energies at each geometry were calculated along with a TD-DFT calculation of 50 singlets and 50 triplets.

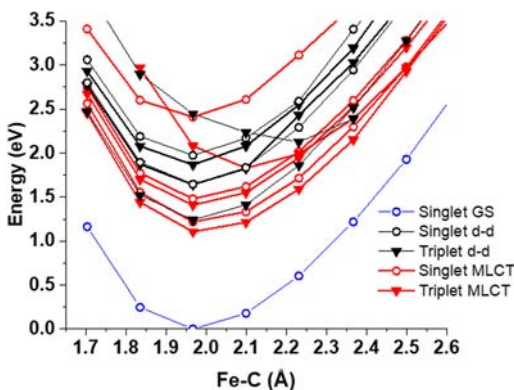


Figure 3: Manifold of states calculated at the Mo6L/6-311g(d) level of theory, with some higher-energy states omitted for clarity. Fe-C displacements are shown.

The results of these calculations are shown in Figure 3, mapped onto the Fe-C stretch coordinate. Each excited state was designated as d-d or MLCT based on analysis of the initial and final orbitals of the highest-contributing transition, as discussed in the computational methods section of the SI. For example, the two lowest  $^3\text{MLCT}$  states are  $d_z^2 \rightarrow N\pi$  and  $d_{xy} \rightarrow N\pi$ . A  $^3\text{MLCT}$  state is calculated to be the lowest excited state, with  $^1\text{MLCT}$  and  $^3\text{MC}$  states 0.113 and 0.135 eV higher in energy, respectively. Along both the Fe-C and Fe-N coordinates, the potentials are well-nested, which discourages intersystem crossing into deactivating MC states from the lowest-energy MLCT state of **1** by elevating or removing the intersections largely responsible for crossing.<sup>31</sup> This is similar to effects observed in the inherently nested spin-flip states of Cr(III) complexes, or sterically-restricted Cu(I) complexes.<sup>32,33</sup>

Orbitals calculated by DFT show the unique effects of HMTI on d-orbital splitting. The Fe-N bond lengths are distributed in diagonally opposing pairs, varying by  $\sim 0.01$  Å adjacently due to the steric influence of the macrocyclic methyl groups. The departure from octahedral to tetragonal symmetry results in an unconventional ligand field, in which  $\pi$ -overlap of the  $\alpha$ -diimines with both the  $d_{yz}$  and  $d_{xz}$  is enabled by the x- and y-axes bisecting the N-Fe-N angles (Figure S11). Thus,  $d_{xy}$  is  $\sigma$ -antibonding with respect to the nitrogen lone pairs, while  $d_{x^2-y^2}$  is nonbonding. These results are consistent with a previous report of the bonding in  $\text{Fe}^{\text{III}}(\text{HMTI})$  systems.<sup>34</sup>

Interestingly, the potential energy surfaces are even steeper along the Fe-N than the Fe-C coordinate. An expansion/contraction of the Fe-N bonds by *ca.* 0.05 Å (Figure S12) results in an increase in energy of  $\geq 1.5$  eV. A simi-

lar change along the Fe-C bonds only increases the energy by *ca.* 0.25 eV. The strong dependence of the energy on the Fe-N geometry is likely a result of the macrocyclic nature of the complex – which inhibits the expansion of the Fe-N bonds frequently associated with metal-centered states.<sup>14,35</sup>

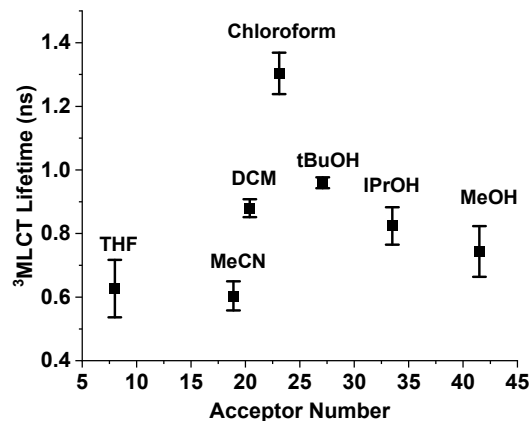
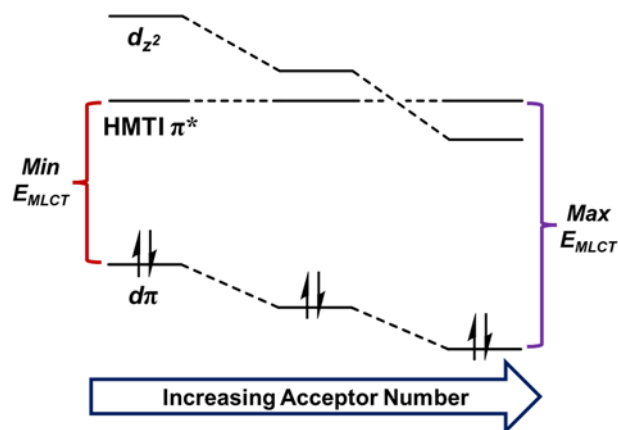


Figure 4: Acceptor number vs. lifetime of the longest-lived MLCT state as observed by OTA.

As shown in Figure 4, the lifetime of the MLCT excited state depends dramatically on the solvent. Moreover, **1** was found to be quite solvatochromic, with the energy of the MLCT band ( $E_{\text{MLCT}}$ ) varying from 1.88 eV (658 nm) in THF up to 2.07 eV (598 nm) in water. Further investigation revealed that this variation exhibited a linear dependence on the Lewis acidity of the solvent (as quantified by the acceptor number,<sup>36</sup> AN; Figure S23). This effect is well documented for charge-transfer states in chromophores bearing cyano ligands,<sup>15,37,38</sup> and results from Lewis acid-base interactions between the solvent and the basic nitrogen of the bound cyanide, as recently described computationally for  $[\text{Fe}(\text{bpy})(\text{CN})_4]^{2-}$  in explicitly modelled  $\text{H}_2\text{O}$ .<sup>39</sup>

In terms of the ligand field, the Lewis acid interaction with the nitrogen base diminishes the electron density on the cyanide ligand. As a result, the  $\sigma/\pi$ -donor character of  $\text{CN}^-$  is reduced, while its  $\pi$ -accepting nature is enhanced.<sup>40-42</sup> (This may be viewed as an intermolecular extension of covalent Lewis acid-cyano adducts which have been recently investigated.<sup>43-45</sup>) The energies of the filled  $d\pi$  and the empty  $d_z^2$  should therefore drop in acidic environments. The energy of the tetraimine  $\pi$  system is expected to stay relatively constant in contrast,<sup>41</sup> so  $E_{\text{MLCT}}$  concomitantly increases (Chart 1), as observed experimentally. This phenomenon allows for the influence of the axial ligand on lifetime to be evaluated.

**Chart 1. Illustration of proposed changes in orbital energies as a function of Lewis acidity.**



Indeed, the lifetimes vary from 627 and 604 ps (THF, AN = 8 and CH<sub>3</sub>CN, AN = 18.9), to 1.25 ns (CHCl<sub>3</sub>, AN = 23.1), to 744 ps (MeOH, AN=41.5). A biphasic pattern emerges in which the lifetime reaches a maximum in environments of intermediate acidity. This has been previously observed for Ru(II)<sup>37</sup> and Fe(II)<sup>5</sup> species bearing cyano ligands, where the phenomenon was attributed to competing deactivation pathways. In solvents of high acceptor number (and therefore higher  $E_{MLCT}$ ), the metal-centered states may become relatively lower in energy, leading to more rapid deactivation.<sup>45</sup> As  $E_{MLCT}$  decreases (with lower AN), deactivation via MC states becomes less significant, but direct deactivation to the ground state increases in accordance with the energy gap law.

However, **1** is distinct from mixed polypyridyl/cyano iron(II) chromophores in that the maximum lifetime achieved is 1.25 ns in CHCl<sub>3</sub> – comparable to the MLCT states of state-of-the art Fe<sup>II</sup> chromophores (e.g. Figure 1, A-C).<sup>9-11</sup> In contrast, the longest MLCT lifetime achieved within a polypyridyl/cyano framework is 67 ps and that of [Fe(bpy)(CN)<sub>4</sub>]<sup>2-</sup> 29 ps.<sup>15</sup> This nearly 20-fold leap in the lifetime of **1** versus its nearest analogues appears to be due to the macrocyclic nature of HMTI, which inhibits expansion of the Fe-N bonds, even in the MC excited states. This results in nested potential energy surfaces, in contrast to typical chelating motifs,<sup>12,14</sup> including [Fe(bpy)(CN)<sub>4</sub>]<sup>2-</sup>.<sup>35</sup>

Indeed, the wide range of lifetimes in various solvents suggests that tuning the donor/acceptor character of the axial ligand should be an effective means of altering the charge-transfer lifetime while maintaining the nested potential surfaces. Furthermore, the nature of  $\pi^*(C=N)$  in Fe(II) tetraimine macrocycles can be readily modified through either the change of double bond locations or the increase in ring unsaturation, which may have profound impact on both the energy and lifetime of the <sup>3</sup>MLCT state. This work suggests that this tetraimine, macrocyclic motif and the nested potentials it creates represent a

hitherto under-explored strategy towards the development of earth abundant alternatives to traditional 4d/5d chromophores.

## ASSOCIATED CONTENT

### Supporting Information

The Supporting Information is available free of charge on the ACS Publications website at DOI:

Synthetic details; TDDFT simulated spectra and molecular orbitals; UV-Vis, IR, <sup>1</sup>H-NMR, and Spectro-electrochemical spectra; Ultrafast TA spectra and kinetic fit details; and geometries used in computational work (PDF)

## AUTHOR INFORMATION

### Corresponding Author

\* Tong Ren – Department of Chemistry, Purdue University, West Lafayette, Indiana 47907, United States; <https://orcid.org/0000-0002-1148-0746>; Email [tren@purdue.edu](mailto:tren@purdue.edu)

\* Josh Vura-Weis – Department of Chemistry, University of Illinois at Urbana-Champaign, Urbana, Illinois 61801, United States; <http://orcid.org/0000-0001-7734-3130>; Email: [vuraweis@illinois.edu](mailto:vuraweis@illinois.edu)

### Authors

Justin Malme – Department of Chemistry, University of Illinois at Urbana-Champaign, Urbana, Illinois 61801  
 Reese A. Clendening – Department of Chemistry, Purdue University, West Lafayette, Indiana 47907, United States  
 Ryan Ash – Department of Chemistry, University of Illinois at Urbana-Champaign, Urbana, Illinois 61801

### Author Contributions

†JM and RAC contributed equally.

### Notes

The authors declare no competing financial interest.

## ACKNOWLEDGMENT

This material is based upon work supported by the National Science Foundation under Grants No. 2102049 to TR and 2102376 to JW. RAC thanks Dr. Matthias Zeller for the data collection of the structure of **1**. We thank Professor James McCusker for insightful suggestions regarding acceptor number correlations.

## REFERENCES

- (1) Wenger, O. S. Photoactive Complexes with Earth-Abundant Metals. *J. Am. Chem. Soc.* **2018**, *140*, 13522-13533.
- (2) Förster, C.; Heinze, K. Photophysics and photochemistry with Earth-abundant metals - fundamentals and concepts. *Chem. Soc. Rev.* **2020**, *49*, 1057-1070.
- (3) McCusker, J. K. Electronic structure in the transition metal block and its implications for light harvesting. *Science* **2019**, *363*, 484-488.
- (4) Grätzel, M. Dye-sensitized solar cells. *J. Photochem. Photobiol. C* **2003**, *4*, 145-153.
- (5) Chan, A. Y.; Perry, I. B.; Bissonnette, N. B.; Buksh, B. F.; Edwards, G. A.; Frye, L. I.; Garry, O. L.; Lavagnino, M. N.;

- Li, B. X.; Liang, Y.; Mao, E.; Millet, A.; Oakley, J. V.; Reed, N. L.; Sakai, H. A.; Seath, C. P.; MacMillan, D. W. C. Metallaphotoredox: The Merger of Photoredox and Transition Metal Catalysis. *Chem. Rev.* **2022**, *122*, 1485-1542.
- (6) Wenger, O. S. Is Iron the New Ruthenium? *Chem. Eur. J.* **2019**, *25*, 6043-6052.
- (7) Dierks, P.; Vukadinovic, Y.; Bauer, M. Photoactive iron complexes: more sustainable, but still a challenge. *Inorg. Chem. Front.* **2022**, *9*, 206-220.
- (8) Chábera, P.; Kjær, K. S.; Prakash, O.; Honarfar, A.; Liu, Y. Z.; Fredin, L. A.; Harlang, T. C. B.; Lidin, S.; Uhlig, J.; Sundström, V.; Lomoth, R.; Persson, P.; Wärnmark, K. Fe-II Hexa N-Heterocyclic Carbene Complex with a 528 ps Metal-to-Ligand Charge-Transfer Excited-State Lifetime. *J. Phys. Chem. Lett.* **2018**, *9*, 459-463.
- (9) Larsen, C. B.; Braun, J. D.; Lozada, I. B.; Kunnus, K.; Biasin, E.; Kolodziej, C.; Burda, C.; Cordones, A. A.; Gaffney, K. J.; Herbert, D. E. Reduction of Electron Repulsion in Highly Covalent Fe-Amido Complexes Counteracts the Impact of a Weak Ligand Field on Excited-State Ordering. *J. Am. Chem. Soc.* **2021**, *143*, 20645-20656.
- (10) Braun, J. D.; Lozada, I. B.; Kolodziej, C.; Burda, C.; Newman, K. M. E.; van Lierop, J.; Davis, R. L.; Herbert, D. E. Iron(II) coordination complexes with panchromatic absorption and nanosecond charge-transfer excited state lifetimes. *Nature Chem.* **2019**, *11*, 1144-1150.
- (11) Leis, W.; Argüello Cordero, M. A.; Lochbrunner, S.; Schubert, H.; Berkefeld, A. A Photoreactive Iron(II) Complex Luminophore. *J. Am. Chem. Soc.* **2022**, *144*, 1169-1173.
- (12) Kjær, K. S.; Kaul, N.; Prakash, O.; Chábera, P.; Rosemann, N. W.; Honarfar, A.; Gordivska, O.; Fredin, L. A.; Bergquist, K.-E.; Häggström, L.; Ericsson, T.; Lindh, L.; Yartsev, A.; Styring, S.; Huang, P.; Uhlig, J.; Bendix, J.; Strand, D.; Sundström, V.; Persson, P.; Lomoth, R.; Wärnmark, K. Luminescence and reactivity of a charge-transfer excited iron complex with nanosecond lifetime. *Science* **2019**, *363*, 249-253.
- (13) Paulus, B. C.; Nielsen, K. C.; Tichnell, C. R.; Carey, M. C.; McCusker, J. K. A Modular Approach to Light Capture and Synthetic Tuning of the Excited-State Properties of Fe(II)-Based Chromophores. *J. Am. Chem. Soc.* **2021**, *143*, 8086-8098.
- (14) Liu, Y. Z.; Kjær, K. S.; Fredin, L. A.; Chábera, P.; Harlang, T.; Canton, S. E.; Lidin, S.; Zhang, J. X.; Lomoth, R.; Bergquist, K. E.; Persson, P.; Wärnmark, K.; Sundström, V. A Heteroleptic Ferrous Complex with Mesoionic Bis(1,2,3-triazol-5-ylidene) Ligands: Taming the MLCT Excited State of Iron(II). *Chem. Eur. J.* **2015**, *21*, 3628-3639.
- (15) Kunnus, K.; Li, L.; Titus, C. J.; Lee, S. J.; Reinhard, M. E.; Koroidov, S.; Kjær, K. S.; Hong, K.; Ledbetter, K.; Doriese, W. B.; O'Neil, G. C.; Swetz, D. S.; Ullom, J. N.; Li, D.; Irwin, K.; Nordlund, D.; Cordones, A. A.; Gaffney, K. J. Chemical control of competing electron transfer pathways in iron tetracyanopolypyridyl photosensitizers. *Chem. Sci.* **2020**, *11*, 4360-4373.
- (16) Clendening, R. A.; Ren, T. Mono- and Bis-alkynyl Iron Complexes Supported by a "Softened" Tetraaza Macrocyclic. *Eur. J. Inorg. Chem.* **2022**, *2022*, e202101021.
- (17) Dabrowiak, J. C.; Lovecchio, F. V.; Goedken, V. L.; Busch, D. H. Synthesis and electrochemical behavior of a new series of macrocyclic complexes of iron produced by oxidative dehydrogenation and tautomerization. *J. Am. Chem. Soc.* **1972**, *94*, 5502-5504.
- (18) Dabrowiak, J. C.; Busch, D. H. Iron complexes with macrocyclic ligands containing the .alpha.-diimine functional unit and its position-specific formation under the influence of the iron atom. *Inorg. Chem.* **1975**, *14*, 1881-1888. Fo
- (19) Lu, T.-H.; Kao, H.-Y.; Wu, D. I.; Kong, K. C.; Cheng, C. H. Structure of Bis(2,2'-bipyridine)dicyanoiron(III) Perchlorate. *Acta Cryst. C* **1988**, *44*, 1184-1186.
- (20) Nieuwenhuyzen, M.; Bertram, B.; Gallagher, J. F.; Vos, J. G. Dipotassium (2,2'-Bipyridyl-*N,N'*)-tetracyanoferrate(II) 2.5-Hydrate, K<sub>2</sub>[Fe(bpy)(CN)<sub>4</sub>].2.5H<sub>2</sub>O. *Acta Cryst. C* **1998**, *54*, 603-606.
- (21) S.-Zhan; Q.-Meng; X.-You; Wang, G.; Zheng, P.-J. The Properties, Crystal and Molecular Structure of *Cis*-Dicyano-Bis(1,10-Phenanthroline)Iron(II) Trihydrate. *Polyhedron* **1996**, *15*, 2655-2658.
- (22) Wang, Y.; Ma, X.; Hu, S.; Wen, Y.; Xue, Z.; Zhu, X.; Zhang, X.; Sheng, T.; Wu, X. Syntheses, crystal structures, MMCT and magnetic properties of four one-dimensional cyanide-bridged complexes comprised of MII-CN-FeIII (M = Fe, Ru, Os). *Dalton Trans.* **2014**, *43*, 17453-17462.
- (23) Brown, A. M.; McCusker, C. E.; McCusker, J. K. Spectroelectrochemical identification of charge-transfer excited states in transition metal-based polypyridyl complexes. *Dalton Trans.* **2014**, *43*, 17635-17646.
- (24) *Gaussian 16 Rev. A.03*; Frisch, M. J.; Trucks, G. W.; Schlegel, H. B.; Scuseria, G. E.; Robb, M. A.; Cheeseman, J. R.; Scalmani, G.; Barone, V.; Petersson, G. A.; Nakatsuji, H.; Li, X.; Caricato, M.; Marenich, A. V.; Bloino, J.; Janesko, B. G.; Gomperts, R.; Mennucci, B.; Hratchian, H. P.; Ortiz, J. V.; Izmaylov, A. F.; Sonnenberg, J. L.; Williams-Yong, D.; Ding, F.; Lipparini, F.; Egidi, F.; Goings, J.; Peng, B.; Peverone, A.; Henderson, T.; Ranasinghe, D.; Zakrzewski, V. G.; Gao, J.; Rega, N.; Zheng, G.; Liang, W.; Hada, M.; Ehara, M.; Toyota, K.; Fukuda, R.; Hasegawa, J.; Ishida, M.; Nakajima, T.; Honda, Y.; Kitao, O.; Nakai, H.; Vreven, T.; Throssell, K.; Montgomery, J. A., Jr.; Peralta, J. E.; Ogliaro, F.; Bearpark, M. J.; Heyd, J. J.; Brothers, E. N.; Kudin, K. N.; Staroverov, V. N.; Keith, T. A.; Kobayashi, R.; Normand, J.; Raghavachari, K.; Rendell, A. P.; Burant, J. C.; Iyengar, S. S.; Tomasi, J.; Cossi, M.; Millam, J. M.; Klene, M.; Adamo, C.; Cammi, R.; Ochterski, J. W.; Martin, R. L.; Morokuma, K.; Farkas, O.; Foresman, J. B.; Fox, D. J.: Wallingford, CT, 2016.
- (25) Neese, F.; Wennmohs, F.; Becker, U.; Riplinger, C. The ORCA quantum chemistry program package. *J. Chem. Phys.* **2020**, *152*, 224108.
- (26) Becke, A. D. Density-functional thermochemistry. III. The role of exact exchange. *J. Chem. Phys.* **1993**, *98*, 5648-5652.
- (27) Raghavachari, K.; Trucks, G. W. Highly correlated systems: Excitation energies of first row transition metals Sc-Cu. *J. Chem. Phys.* **1989**, *91*, 1062-1065.
- (28) Hay, P. J. Gaussian basis sets for molecular calculations - representation of 3D orbitals in transition-metal atoms. *J. Chem. Phys.* **1977**, *66*, 4377-4384.
- (29) Wachters, A. J. H. Gaussian basis set for molecular wavefunctions containing third-row atoms. *J. Chem. Phys.* **1970**, *52*, 1033.
- (30) Cossi, M.; Rega, N.; Scalmani, G.; Barone, V. Energies, structures, and electronic properties of molecules in solution with the C-PCM solvation model. *J. Comp. Chem.* **2003**, *24*, 669-681.
- (31) Kjær, K. S.; Van Driel, T. B.; Harlang, T. C. B.; Kunnus, K.; Biasin, E.; Ledbetter, K.; Hartsock, R. W.; Reinhard, M. E.; Koroidov, S.; Li, L.; Laursen, M. G.; Hansen, F. B.; Vester, P.; Christensen, M.; Haldrup, K.; Nielsen, M. M.; Dohn, A. O.; Pappai, M. I.; Moller, K. B.; Chábera, P.; Liu, Y. Z.; Tatsuno, H.; Timm, C.; Jarenmark, M.; Uhlig, J.; Sundstom, V.; Wärnmark, K.; Persson, P.; Nemeth, Z.; Szemes, D. S.; Bajnaczi, E.; Vanko, G.; Alonso-Mori, R.; Glowina, J. M.; Nelson, S.; Sikorski, M.; Sokaras, D.; Canton, S. E.; Lemke, H. T.; Gaffney, K. J. Finding

- intersections between electronic excited state potential energy surfaces with simultaneous ultrafast X-ray scattering and spectroscopy. *Chem. Sci.* **2019**, *10*, 5749-5760.
- (32) Otto, S.; Dorn, M.; Förster, C.; Bauer, M.; Seitz, M.; Heinze, K. Understanding and exploiting long-lived near-infrared emission of a molecular ruby. *Coord. Chem. Rev.* **2018**, *359*, 102-111.
- (33) Mara, M.; Fransted, K.; Chen, L. Interplays of excited state structures and dynamics in copper(I) diimine complexes: Implications and perspectives. *Coord. Chem. Rev.* **2015**, *282-283*, 2-18.
- (34) Clendening, R. A.; Zeller, M.; Ren, T. Bis-Alkynyl Complexes of Fe(III) Tetraaza Macrocycles - A Tale of Two Rings. *Inorg. Chem.* **2022**, *61*, 13442-13452.
- (35) Zhang, W. K.; Kjær, K. S.; Alonso-Mori, R.; Bergmann, U.; Chollet, M.; Fredin, L. A.; Hadt, R. G.; Hartsock, R. W.; Harlang, T.; Kroll, T.; Kubiček, K.; Lemke, H. T.; Liang, H. W.; Liu, Y. Z.; Nielsen, M. M.; Persson, P.; Robinson, J. S.; Solomon, E. I.; Sun, Z.; Sokaras, D.; van Driel, T. B.; Weng, T. C.; Zhu, D. L.; Wärnmark, K.; Sundström, V.; Gaffney, K. J. Manipulating charge transfer excited state relaxation and spin crossover in iron coordination complexes with ligand substitution. *Chem. Sci.* **2017**, *8*, 515-523.
- (36) Mayer, U.; Gutmann, V.; Gerger, W. The Acceptor Number - A Quantitative Empirical Parameter for the Electrophilic Properties of Solvents. *Monatsh. Chem.* **1975**, *106*, 1235-1257.
- (37) Indelli, M. T.; Bignozzi, C. A.; Scandola, F.; Collin, J.-P. Design of Long-Lived Ru(II) Terpyridine MLCT States. Tricyano Terpyridine Complexes. *Inorg. Chem.* **1998**, *37*, 6084-6089.
- (38) Soukup, R. W.; Schmid, R. Metal Complexes as Color Indicators for Solvent Parameters. *J. Chem. Ed.* **1985**, *62*, 459-462.
- (39) Zederkof, D. B.; Møller, K. B.; Nielsen, M. M.; Haldrup, K.; González, L.; Mai, S. Resolving Femtosecond Solvent Reorganization Dynamics in an Iron Complex by Nonadiabatic Dynamics Simulations. *J. Am. Chem. Soc.* **2022**, *144*, 12861-12873.
- (40) Kjær, K. S.; Kunnus, K.; Harlang, T. C. B.; Van Driel, T. B.; Ledbetter, K.; Hartsock, R. W.; Reinhard, M. E.; Koroidov, S.; Li, L.; Laursen, M. G.; Biasin, E.; Hansen, F. B.; Vester, P.; Christensen, M.; Haldrup, K.; Nielsen, M. M.; Chábera, P.; Liu, Y. Z.; Tatsuno, H.; Timm, C.; Uhlig, J.; Sundstom, V.; Nemeth, Z.; Szemes, D. S.; Bajnoczi, E.; Vanko, G.; Alonso-Mori, R.; Glownia, J. M.; Nelson, S.; Sikorski, M.; Sokaras, D.; Lemke, H. T.; Canton, S. E.; Wärnmark, K.; Persson, P.; Cordones, A. A.; Gaffney, K. J. Solvent control of charge transfer excited state relaxation pathways in Fe(2,2'-bipyridine)(CN)(4) (2-). *PCCP* **2018**, *20*, 4238-4249.
- (41) Timpson, C. J.; Bignozzi, C. A.; Sullivan, B. P.; Kober, E. M.; Meyer, T. J. Influence of Solvent on the Spectroscopic Properties of Cyano Complexes of Ruthenium(II). *J. Phys. Chem.* **1996**, *100*, 2915-2925.
- (42) Jay, R. M.; Vaz da Cruz, V. c.; Eckert, S.; Fondell, M.; Mitzner, R.; Föhlisch, A. Probing Solute-Solvent Interactions of Transition Metal Complexes Using L-Edge Absorption Spectroscopy. *J. Phys. Chem. B* **2020**, *124*, 5636-5645.
- (43) Ngo, D. X.; Del Ciello, S. A.; Barth, A. T.; Hadt, R. G.; Grubbs, R. H.; Gray, H. B.; McNicholas, B. J. Electronic Structures, Spectroscopy, and Electrochemistry of [M(diimine)(CN-BR<sub>3</sub>)<sub>4</sub>]<sup>2-</sup> (M = Fe, Ru; R = Ph, C<sub>6</sub>F<sub>5</sub>) Complexes. *Inorg. Chem.* **2020**, *59*, 9594-9604.
- (44) Schmid, L.; Kerzig, C.; Prescimone, A.; Wenger, O. S. Photostable Ruthenium(II) Isocyanoborato Luminophores and Their Use in Energy Transfer and Photoredox Catalysis. *JACS Au* **2021**, *1*, 819-832.
- (45) Schmid, L.; Chábera, P.; Ruter, I.; Prescimone, A.; Meyer, F.; Yartsev, A.; Persson, P.; Wenger, O. S. Borylation in the Second Coordination Sphere of FeII Cyanido Complexes and Its Impact on Their Electronic Structures and Excited-State Dynamics. *Inorg. Chem.* **2022**, *61*, 15853-15863.

SYNOPSIS TOC: The constricted geometry of a tetragonal Fe<sup>II</sup> macrocyclic complex results in a unique set of nested potentials, which permits access to nanosecond charge-transfer lifetimes in the appropriate medium. These lifetimes depend strongly on the interactions between the cyano axial ligands and the solvent environment.

**For Table of Contents Only:**

